JARQ 54 (1), 101-112 (2020) https://www.jircas.go.jp

Vegetation Dynamics and Phenological Shifts in Long-term NDVI Time Series in Inner Mongolia, China

Zhe GONG[1], Kensuke KAWAMURA[2]*, Naoto ISHIKAWA[3], Masakazu GOTO[4], Wulan TUYA[5], Dalai ALATENG[6], Ting YIN[7] and Yutaka ITO[8]

[1] Graduate School for International Development and Cooperation, Hiroshima University, Higashi-Hiroshima, Japan
[2] Social Sciences Division, Japan International Research Center for Agricultural Science, Tsukuba, Japan
[3] Faculty of Food and Agricultural Sciences, Fukushima University, Fukushima, Japan
[4] Faculty of Bioresources, Mie University, Tsu, Japan
[5] Rangeland Survey and Design Institute of Inner Mongolia, Inner Mongolia Autonomous Region Office of Agriculture and Animal Husbandry, Huhhot, Inner Mongolia, China
[6] Biotechnology Research Center, Inner Mongolia Academy of Agricultural and Animal Husbandry Sciences, Huhhot, Inner Mongolia, China
[7] Research Institute of Economy, Trade and Industry, Chiyoda-ku, Tokyo, Japan
[8] Faculty of International Resource Sciences, Akita University, Akita, Japan

Abstract

To assess the dynamics of vegetation growth and phenology in the Inner Mongolia Autonomous Region in China, a time series of Normalized Difference Vegetation Index (NDVI) data from 1983 to 2013, derived from the Advanced Very High-Resolution Radiometer-Vegetation Health Product (AVHRR-VHP), was applied to detect linear trends, seasonal phenology transition dates, and growing seasons. Overall, Inner Mongolia became warmer and drier during the study period. A significant increasing cumulative NDVI trend was found for 30.30% of the total vegetation covered area. The restored area was mainly in the western desert steppe. The degraded area was primarily located in the northeastern meadow and typical steppe regions. However, a severe drought was detected during 1993-2003, when approximately 27.56% of the total vegetation covered area experienced a significant decreasing NDVI trend. The length of the growing season (LOS) during 1983-2013 was shortened due to the delayed start of the growing season (SOS) and advanced timing of the end of the growing season (EOS). However, this trend was reversed during the more recent decade (2003-2013). The phenology was closely associated with climate change, especially precipitation. The variability of vegetation responses to climate change was also assessed, indicating that most types of vegetation had recently recovered and that the restored areas had a varied spatial distribution.

Discipline: Animal Science
Additional key words: cumulative annual NDVI, heterogenous distribution, land degradation, vegetation recovery

Introduction

Land degradation has long been considered a global environmental issue (Gisladottir & Stocking 2005, Kröpfl et al. 2013, Ravi et al. 2010, Rey et al. 2011, Sop & Oldeland 2013). The Inner Mongolia Autonomous Region (IMAR) of China, one of the largest grasslands in the world, has suffered from severe degradation for a long time (Jiang et al. 2006). The Inner Mongolian grassland supports a large population of sheep, goats, cattle and other herbivores, providing the main economic benefit for the local community (Ellis 1992, Lee et al. 2002). Land degradation causes declines in soil quality, resulting in dramatic changes in the vegetation. The loss of vegetation cover makes the soil more sensitive to erosion (Ravi et al. 2010). Thus, studies of vegetation patterns and responses to external influences are necessary to control land degradation.

*Corresponding author: e-mail kamuken@affrc.go.jp
Received 5 November 2018; accepted 25 June 2019.

Remote sensing technology is widely accepted as the most effective tool for monitoring the growth of vegetation over large spatial scales. The vegetation indices derived from various satellite sensors can provide a continual source of high spatial- and temporal-resolution data. Normalized Difference Vegetation Index (NDVI) data are the most popular for identifying the long-term trends and phenology of vegetation (Jeong et al. 2011, Kawamura et al. 2005, Piao et al. 2006, Wu & Liu 2013). Previous studies found that the start of the vegetative growing season was early (advanced) in the IMAR due to climate change, such as in precipitation and temperature (Cong et al. 2013). Longer growing seasons, including earlier spring vegetation greening, significantly enhance the vegetation productivity in temperate and boreal regions (Hu et al. 2010, Kimball et al. 2004).

The growth of vegetation is greatly affected by climate change and human activities (Li et al. 2012). However, these dominant factors change over time. Some researchers have indicated that the IMAR has become warmer and drier (Ding & Chen 2008). However, our previous study using an NDVI time series obtained by the Terra Moderate Resolution Imaging Spectroradiometer (MODIS) during 2002-2014 (Gong et al. 2015) indicated that the IMAR became wetter and colder during those years, and that the rate of advance (forward movement) of the growing season was also more gradual than that found in previous research. Moreover, the effects of human activity varied during these years. Changes in land use policy, overstocking, and uneven grazing increased the stress on vegetation in the IMAR (Li et al. 2007, Ludwig et al. 2000). In an effort to reverse land degradation, the Chinese government established the "Grain for Green" program in 1999 for restoring the vegetation and recovering ecosystems (Zhou et al. 2009). Earlier studies have reported that the vegetation in Inner Mongolia was recently restored (Yong-Zhong et al. 2005, Zhan et al. 2007). However, the heterogeneous spatial distribution of the recovered areas also suggested that additional efforts are needed to reveal the reasons for this pattern and develop effective recovery technologies (Miao et al. 2015). Most existing studies have investigated vegetation change over relatively short time periods using data from historical periods or recent years, which are insufficient for the discovery of long-term dynamics. Thus, longer study periods are necessary to explore the continual changes in vegetative activity and consider the effects of human activities and climate change. The NDVI time series derived from the Advanced Very High-Resolution Radiometer-Vegetation Health Product (AVHRR-VHP), developed by the Center for Satellite Applications and Research (STAR) at the National Oceanic and Atmospheric Administration (NOAA), provides an NDVI time series for the longest period (from 1981 to the present). Thus, the shifts in vegetation growth can be detected in different stages across the years. Three decades (1983-1993, 1993-2003, and 2003-2013) were delineated to assess the responses of various vegetation types to climate change and social effects, such as before and after implementation of the "Grain for Green" program.

The objectives of this study are to: (1) detect the trends in vegetative activity and the phenological shifts in the IMAR using the NDVI derived from NOAA's AVHRR-VHP (1983-2013), (2) assess the interrelationships between the phenological shifts and climate dynamics, and (3) compare the response of various vegetation types to climate change over three different periods.

Materials and methods

1. Study area

The IMAR (Fig. 1), located in the northern part of China, is a typical arid and semi-arid region that occupies a total area of 1.18 million km^2 (John et al. 2008). This region exhibits large climate gradients and various land use types. Five dominant vegetation cover types in the IMAR (i.e., forest, meadow steppe, typical steppe, desert steppe, Gobi Desert) were detected (Zhang 2007). The mean annual precipitation is concentrated in June and July, with more than 400 mm in the northeastern forests and less than 100 mm in the western Gobi Desert (John et al. 2008, Yu et al. 2003, Zhao et al. 2006). The yearly average temperature ranges between 0 and 8°C. The typical meadow and desert steppes in the central region are the major grassland ecosystem types in the IMAR. Thus, grazing and animal husbandry are often found in this area. The meadow steppe has the highest productivity, with annual precipitation of approximately 400 mm. The primary plant species are *Stipa baicalensis*, *Leymus chinensis*, and *Cleistogenes mucronata* (Gong et al. 2015, John et al. 2008, Kang et al. 2007). In the semi-arid typical steppe where annual precipitation is less than 300 mm, the dominant plant species are *S. grandis*, *L. chinensis*, and multiple species of *Artemisia* spp. and *Festuca* spp. (Kang et al. 2007, Gong et al. 2015, Yu et al. 2003). The desert steppe has the lowest biomass production and is located in an arid area, where annual precipitation is always less than 200 mm. The dominant plant species in the desert steppe are *S. krylovii*, *S. bungeana*, and *A. ordosica* (John et al. 2008, Kang et al. 2007, Yu et al. 2003). The forest area in the northeast is rich in biomass and has the highest precipitation, but the lowest temperature compared with the other ecosystems.

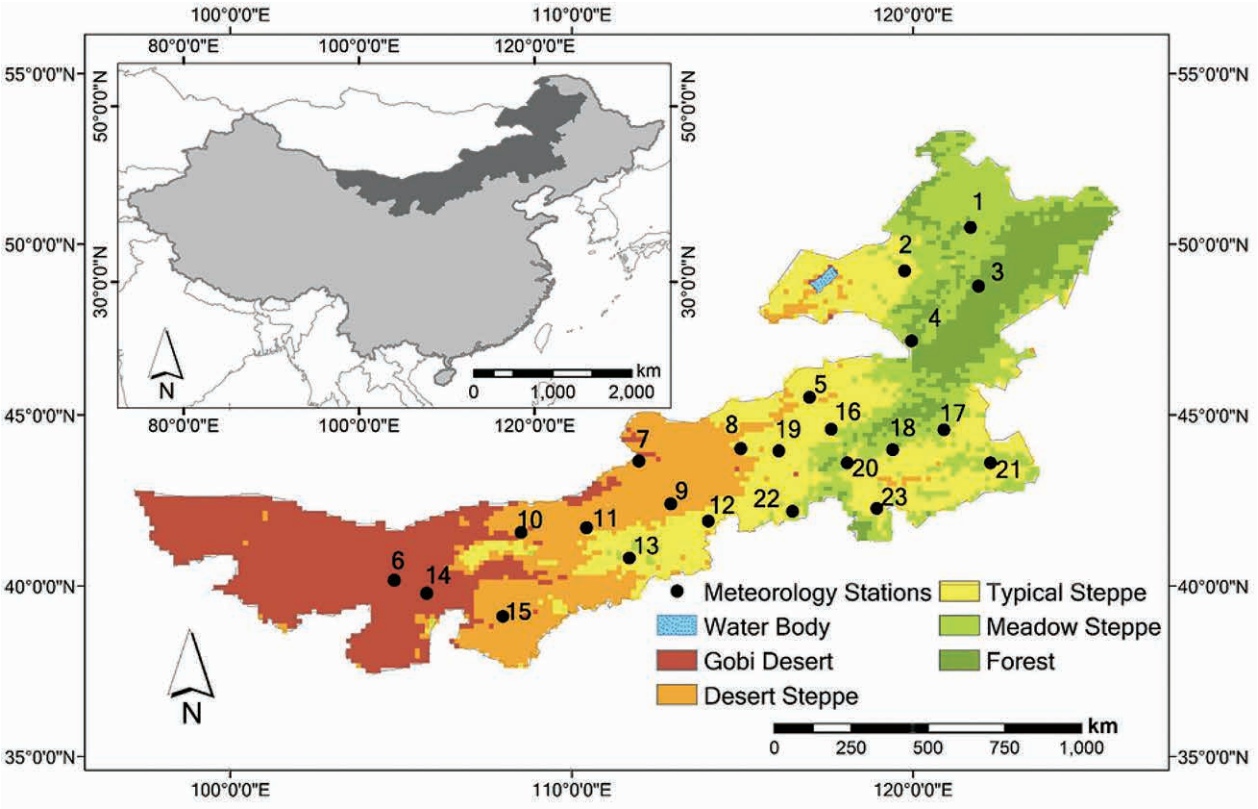

Fig. 1. Locations and vegetation cover types in the Inner Mongolia Autonomous Region (IMAR) of China
Black dots denote locations of the 23 meteorological stations (see Table 1).

The Gobi Desert area in the west seldom receives annual precipitation greater than 150 mm.

2. Data sources

The meteorological data on Inner Mongolia were provided by the China Meteorological Data Sharing Service System (http://www.escience.gov.cn/metdata/page/index.html). Twenty-three meteorological stations (Fig. 1 and Table 1) across the IMAR were selected to represent forest, meadow steppe, typical steppe, desert steppe, and Gobi Desert areas. Based on the land cover types in Inner Mongolia (Editorial Board of Vegetation Map of China and Chinese Academy of Sciences 2007), we divided the vegetation types of the 23 total meteorological stations into five dominant types, listed in Table 1 as follows: forest (n = 2), meadow steppe (n = 5), typical steppe (n = 8), desert steppe (n = 6) and Gobi Desert (n = 2).

The NDVI time series from 1983 to 2013 derived from NOAA's AVHRR-VHP (a weekly product with spatial resolution of 16 km) was applied to evaluate vegetative growth (http://www.star.nesdis.noaa.gov/smcd/emb/vci/VH/vh_ftp.php). The NDVI is a nonlinear combination of red and near-infrared (NIR) spectral radiances (NIR − red)/(NIR + red) that reflects vegetative activity and green biomass. The index is usually employed for assessing phenology from space (Glenn et al. 2008, Hmimina et al. 2013, Karlsen et al. 2008). The NDVI time series was composited using the data detected by NOAA 7, 9, 11, 14, 16, 18, and 19 aboard different platforms.

3. Reconstruction of the NDVI time series

The raw NDVI data were smoothed using the Empirical Distribution Function (EDF) method (Crosby et al. 1996). Quality assessment (QA) was used to determine the acceptable NDVI values; the invalid NDVI values with QA = 0 or 1 were omitted and interpolated linearly.

Due to the noise caused by other factors (e.g., thin clouds), however, the NDVI time series needed to be smoothed again. The Savitzky-Golay filter (Chen et al. 2004) is a popular smoothing method that can be explained by the function expressed as follows:

$$Y_j^* = \frac{\sum_{i=-m}^{i=m} C_i Y_{j+i}}{N} \quad (1)$$

where Y is the original NDVI value, Y^* the resultant NDVI value, and Ci the coefficient for the ith NDVI of the smoothing window (Chen et al. 2004). N is the number

Table 1. Meteorological station information (1981-2010)

No.	Station name	Vegetation type	Elevation (m)	Annual mean precipitation (mm)	Mean temperature (°C)
1	Tulihe	MS	732.6	450.46	−4.04
2	Hailaer	MS	610.2	357.53	−0.47
3	Boketu	Forest	739.7	476.81	−0.12
4	Aershan	Forest	1,027.4	451.86	−2.31
5	Dongwuzhumuqin	TS	838.7	253.03	1.97
6	Bayanmaodao	Gobi Desert	1,323.9	106.31	7.70
7	Erlianhot	DS	964.7	135.04	4.66
8	Abagaqi	DS	1,126.1	237.57	1.97
9	Zhurihe	DS	1,150.8	202.42	5.52
10	Wulatezhongqi	DS	1,288.0	204.81	5.84
11	Daerhanlianheqi	DS	1,376.6	253.06	4.76
12	Huade	TS	1,482.7	317.84	3.25
13	Huhhot	TS	1,063.0	399.87	7.40
14	Jilantai	Gobi Desert	1,031.8	101.49	9.47
15	Etuokeqi	DS	1,380.3	267.64	7.54
16	Xiwuzhumuqin	TS	1,000.6	329.74	2.01
17	Zhaluteqi	MS	265.0	376.46	7.07
18	Balinzuoqi	MS	484.4	379.97	5.94
19	Xilinhot	TS	989.5	269.48	3.01
20	Linxi	TS	799.0	373.53	5.15
21	Tongliao	MS	178.5	368.07	7.10
22	Duolun	TS	1,245.4	376.57	2.80
23	Chifeng	TS	568.0	374.35	7.71

MS: meadow steppe, TS: typical steppe, DS: desert steppe

of convoluting integers and equal to the smoothing window size ($2m + 1$). j represents the running index of ordinate data in the original data table, and m represents the half width of the smoothing window (Savitzky & Golay 1964). The two main parameters that determine the final output are the half width of the smoothing window (m) and the degree of the filtering polynomial (d). In this study, m was set to 4 and d to 2, so as to obtain the best fitting result. The two assumptions which must be confirmed are that the time series follows an annual cycle of growth and decline, and that clouds and poor atmospheric conditions decrease the NDVI values. Therefore, sudden decreases in the NDVI that are not compatible with the gradual process of vegetation change should be regarded as noise and removed.

In the NDVI image, 6,271 pixels were determined to represent the Inner Mongolia area; 6,262 pixels represented land, and the other 9 pixels covered water (NDVI = −999, same as the invalid areas). The mean cumulative AVHRR NDVI values were classified into five levels (less than 0.1, 0.1-0.15, 0.15-0.2, 0.2-0.25, and greater than 0.25), corresponding to the Gobi Desert, desert steppe, typical steppe, meadow steppe, and forest biome (Fig. 1). These thresholds values were set to match the vegetation map of the People's Republic of China (Zhang 2007). As the vegetation is rarely distributed in the Gobi Desert (mean NDVI < 0.1), only the NDVI time series data for the areas covered with vegetation (4,928 pixels) were used for calculations.

Using the smoothed NDVI time series data (1,563 values/pixel from 1983 to 2013), linear models were developed to obtain the trends of the data set. The positive and negative slopes of the models represent increasing and decreasing trends, respectively. The slopes were tested at a significance level of 5% ($P < 0.05$). Subsequently, the F significance test was used to mask the pixels with a significance level of less than 0.05.

4. Phenology determination

Various methods have been applied to detect

phenological shifts using the NDVI time series (Cong et al. 2013, Vrieling et al. 2011, Wu & Liu 2013). In the present study, the start of the growing season (SOS) was set as the date when the second derivative reached the highest value in spring (from March to June). The peak of growing activity in the season (POS) was set as the time when the NDVI reached the highest value during the study period. The end of the growing season (EOS) was determined as the time when the second derivative reached the highest value in autumn (from July to October). The length of the growing season (LOS) was the period between the start and end of the growing season. The relationships between the phenology dates (SOS, POS, EOS, and LOS) and meteorological data (monthly cumulative precipitation and mean temperatures) were assessed using the population regression function. We developed a simple linear regression model with the phenology date as response variable (y) and meteorological data as explanatory variable (x). Here, the previous year's rainfall and other parameters were also compared as x-variable. The coefficient of determination (R^2) and significance (p) were calculated to compare the correlations between parameters. Further details are given in Gong et al. (2015).

Satellite image processing was conducted using Interactive Data Language (IDL) ver. 8.3 (Exelis Visual Information Solutions, Boulder, Colorado, USA). The correlation analysis was performed using MATLAB software ver. 7.12 (MathWorks Inc., Sherborn, USA). The thematic maps were developed using ArcGIS ver. 10.2.2 (ESRI, California, USA).

Results

1. Climate change

According to the meteorological data collected from 1983 to 2013 by the 23 meteorological stations distributed across the IMAR (Fig. 1), annual precipitation tended to decrease, whereas mean temperature tended to increase (Table 2). Annual precipitation reached a maximum in 1998 (312.84 mm year^{-1}) and a minimum in 2007 (164.37 mm year^{-1}). The mean temperature was 1.92°C in 1985 and 4.08°C in 2007. Over the 31 years, annual precipitation varied considerably at different stations, with the standard derivation (SD) ranging from 114.23 mm year^{-1} to 239.95 mm year^{-1}.

To assess the responses of various vegetation types to climate change and social effects (before and after implementation of the "Grain for Green" program), the meteorological data was divided into three decades (1983-1993, 1993-2003, and 2003-2013) (Table 2). During 1983-1993, both annual precipitation and mean temperature showed increasing trends. During 1993-2003, annual precipitation dramatically decreased, whereas mean temperature continued to exhibit a rising trend. Conversely, during 2003-2013, annual precipitation increased again, but mean temperature decreased.

2. Cumulative NDVI trends

Figure 2 and Table 3 show the cumulative NDVI trends over different periods. During 1983-2013 (Fig. 2 a), most of the area with significant change had an increasing NDVI trend (30.30% of the vegetation covered area), whereas 21.21% had a decreasing NDVI. The decreased NDVI area was primarily located in the meadow steppe and typical steppe in the northeastern and central parts of the IMAR. Some of the western desert steppe also exhibited a decreased NDVI. The northeastern forest and western desert steppe regions showed an increasing NDVI trend.

During 1983-1993 (Fig. 2 b), some areas of the typical steppe region tended to exhibit increasing NDVI trends. The northern desert steppes and some meadow steppe areas exhibited significantly decreasing NDVI trends. In the driest decade (1993-2003) (Fig. 2 c), the largest area (27.56%) was obviously degraded, except for some forest and desert steppe areas. Then during 2003-2013 (Fig. 2 d), the cumulative NDVI trend in the northeastern meadow steppe and most of the western desert steppe increased (18.28%). Only 4.65% of the vegetation covered area exhibited a downward NDVI trend, primarily the typical and meadow steppes in the central region and some arid areas.

During the study period, the vegetation decreased most significantly during 1993-2003. The cumulative NDVI in the forest area remained the most stable

Table 2. Annual precipitation and mean monthly temperature trends for different periods

Variable		1983-1993	1993-2003	2003-2013	1983-2013
Precipitation	Slope	2.04	−4.65	4.65	−0.91
	Intercept	229.19	257.72	190.31	242.45
Temperature	Slope	0.07	0.04	−0.06	0.03
	Intercept	2.22	2.96	3.60	2.61

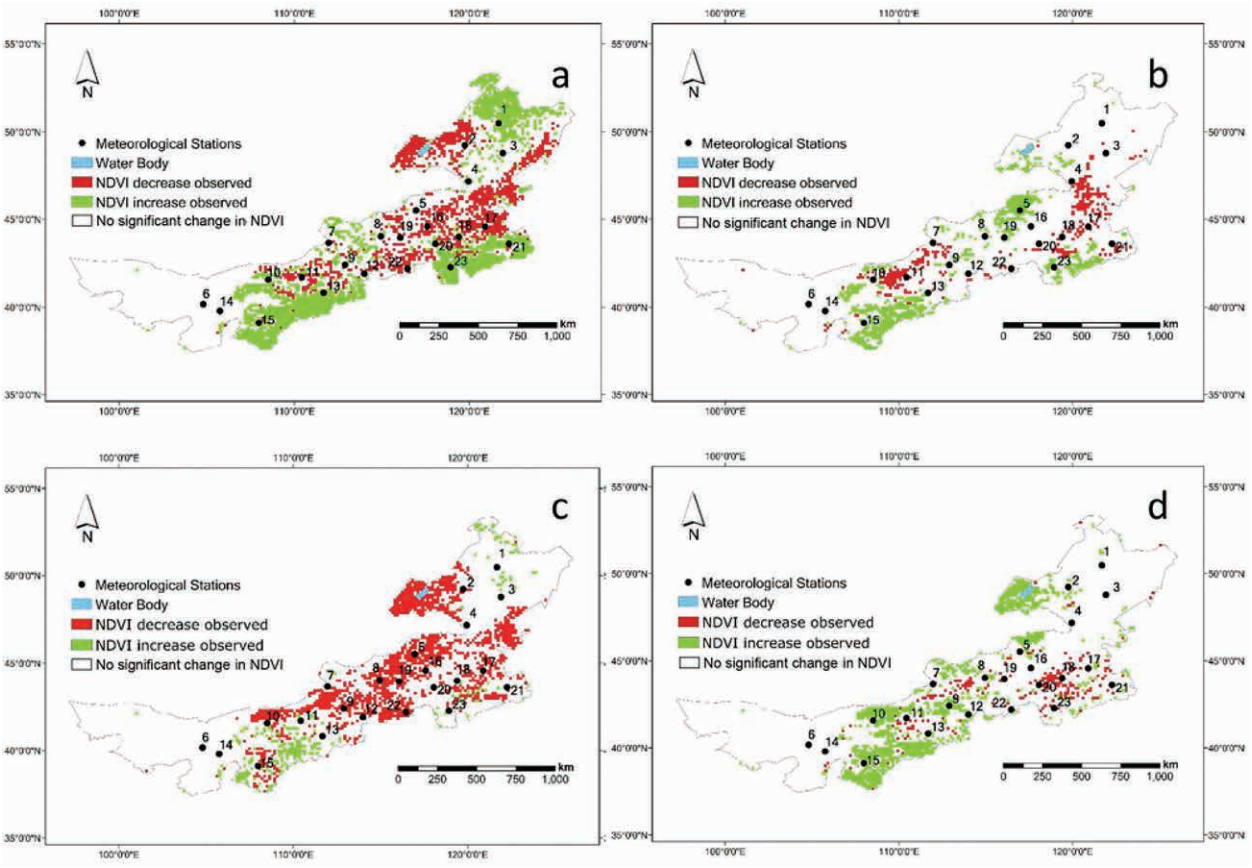

Fig. 2. Cumulative NDVI trends: (a) 1983-2013, (b) 1983-1993, (c) 1993-2003, and (d) 2003-2013
Red, green, and white areas denote areas with decreasing, increasing, and no significant change in NDVI trends (slopes), respectively.

Table 3. Areas with increasing, decreasing, and no significant change of cumulative NDVI trends for different periods, and percent ratios of the whole area (%)

Variable	1983-1993	1993-2003	2003-2013	1983-2013
Area NDVI Increased ($\times 10^4$ km^2)	16.54 (13.11%)	6.35 (5.03%)	23.07 (18.28%)	38.22 (30.30%)
Area NDVI Decreased ($\times 10^4$ km^2)	8.29 (6.57%)	34.76 (27.56%)	5.86 (4.65%)	26.75 (21.21%)
No Significant Change Area ($\times 10^4$ km^2)	101.32 (80.32%)	85.04 (67.41%)	97.23 (77.07%)	61.18 (48.50%)

compared with the other vegetation types. The cumulative NDVI of the western desert steppe increased recently, meaning that vegetative activity was promoted in the arid areas of Inner Mongolia. However, the NDVI trend of the typical and meadow steppes was distributed unequally, reflecting heterogeneous vegetation recovery in the semi-arid areas.

3. Phenology dynamics

Based on the seasonal phenology transition dates (SOS, POS, EOS, and LOS) of all 23 meteorological stations, the mean SOS of all stations in the study period ranged from May to early June, with a mean value of 144.69 ± 10.13 day of year (DOY), where 10.13 was the SD of the mean annual SOS. The SD of stations ranged from 15.79 days in 2010 to 37.32 days in 1998, showing that the SOS varied significantly within the regions with different vegetation types and climatic conditions. The POS appeared in July and August, with the mean annual value of 218.76 ± 5.84 DOY. The EOS occurred from mid-September to October, with a mean annual value of 279.60 ± 7.30 DOY. The mean annual LOS was 135.92 ±

14.29 days. The LOS exhibited the greatest mean SD of stations (46.20 days), indicating a significant spatially heterogeneous distribution of phenology across vast Inner Mongolia.

According to the linear model shown in Table 4, during the entire monitoring period (1983-2013), the SOS was postponed by 5.40 days (= 0.18 day/year × 30 years), whereas the POS and EOS were advanced by 2.10 days (= −0.07 day/year × 30 years) and 6.00 days (= −0.20 day/year × 30 years), respectively. Thus, the LOS had been shortened by 11.70 days (= −0.39 day/year × 30 years). The SOS was postponed during 1983-1993 but continually advanced, especially during 2003-2013, when it was advanced by 12.80 days. The LOS decreased until 1993-2003. These changes suggest strong vegetation growth during 2003-2013.

4. Correlations between climate and phenological dynamics, 1983-2013

As shown in Table 5, the SOS was correlated negatively with the cumulative autumn precipitation from September to October, with the highest correlation in the previous year (R^2 = 0.35, P < 0.05) of these 31 years. Moreover, the SOS had a positive relationship with the mean April temperature in the previous year (R^2 = 0.33, P < 0.05). The increase in precipitation and colder spring temperatures may advance the SOS, but correlations between climate and POS were not significantly detected here. A decrease in precipitation from September to November in the previous year and an increase in temperature in March of the previous year helped the POS advance. The EOS was positively correlated with the autumn precipitation from August to September (R^2 =

Table 4. Slope and intercept from linear fittings of yearly changes in phenology transition dates during different periods

Variable		1983-1993	1993-2003	2003-2013	1983-2013
SOS	Slope	0.01	−0.01	−1.28	0.18
	Intercept	141.07	145.73	154.53	141.75
POS	Slope	−0.70	−1.00	−0.53	−0.07
	Intercept	222.45	225.22	221.71	219.93
EOS	Slope	−0.29	−0.21	−0.18	−0.20
	Intercept	284.36	278.71	279.47	282.87
LOS	Slope	−0.30	−0.21	1.10	−0.39
	Intercept	144.29	133.98	125.94	142.13

SOS is the start of the growing season; POS is the maximum NDVI date during the growing season; EOS is the end of the growing season; LOS is the length of the growing season.

Table 5. Linear models representing correlations between phenology transition dates and climate variables during 1983-2013

Phenology	Variable	Period	Slope	Intercept	R^2	P
SOS	Prec.	September-October (previous year)	−1.34	192.18	0.35	<0.05
	Temp.	April (previous year)	49.45	177.07	0.33	<0.05
POS	Prec.	September-November (previous year)	0.21	172.32	0.18	<0.05
	Temp.	March (previous year)	−2.66	176.79	0.15	<0.05
EOS	Prec.	August-September	1.16	161.94	0.87	<0.001
	Temp.	March	28.61	372.83	0.43	<0.05
LOS	Prec.	February-March	9.89	64.02	0.56	<0.01
	Temp.	June (previous year)	−58.93	1,281.80	0.34	<0.01

SOS is the start of the growing season; POS is the maximum NDVI date during the growing season; EOS is the end of the growing season; LOS is the length of the growing season. Prec. and Temp. denote precipitation and temperature, respectively.

0.87, $P < 0.001$) and with the temperature in March ($R^2 = 0.43$, $P < 0.05$). The decreased precipitation in early autumn and increased spring temperature likely advanced the EOS. The LOS was positively correlated with the spring precipitation from February to March ($R^2 = 0.56$, $P < 0.01$) and negatively correlated with the temperature in June of the previous year ($R^2 = 0.34$, $P < 0.01$). The increased spring precipitation may have promoted vegetation growth, leading to a prolonged growing season.

Discussion

This study detected the cumulative annual NDVI trends and shifts in phenology during the growing season in the IMAR over 31 years. The vegetative activity decreased in most of the areas during 1993-2003, but the trend was reversed during 2003-2013. The phenology dynamics were closely related to climate variations, especially that of precipitation.

1. Cumulative NDVI trends over different time periods

The most significant degenerated cumulative NDVI trend was detected for 1993-2003 (Fig. 2 c). Precipitation and temperature are the main constraints on vegetation growth, and the vegetation in arid and semi-arid regions is quite sensitive to the quantity, timing, and frequency of precipitation (Fan et al. 2016, Gamon et al. 2013, Li et al. 2013). Tian et al. (2015) suggested that annual precipitation most strongly and significantly limited vegetation growth over 45.1% of the IMAR. During 1993-2003, annual precipitation measured by the meteorological stations decreased by 46.5 mm and the mean temperature increased by 0.4°C. Previous research indicated that temperature in the IMAR increased significantly after the mid-1980s (Ding & Chen 2008). Increased temperature can accelerate water evaporation and lead to insufficient soil moisture for vegetation growth. Conversely, the IMAR became wetter and colder after 2003. Similar variations have been discovered by other researchers (Fan et al. 2016, Tian et al. 2015). The cumulative NDVI increased primarily in regions with low biomass (desert steppe) and some parts of the typical and meadow steppes. The typical and meadow steppes in the eastern and central parts of the IMAR degraded significantly. Thus, although the vegetation was generally restored in the IMAR, the areas with rich biomass still suffered from degradation.

2. Linking the phenological shifts and climate change

The SOS became earlier starting in 1993, whereas the EOS advanced throughout all study periods (Table 4). Only the LOS was longer during 2003-2013 because the advance in SOS was greater than the advance in EOS. All phenological shifts were closely related to climate change, especially precipitation. The time lag effects discussed in previous works (Chuai et al. 2013, Cui & Shi 2010, Luo et al. 2009, Xu et al. 2010) were also detected in the present study. The precipitation and temperature during the previous year may strongly affect vegetation growth in the current year, whereas an increasing rate of precipitation can promote vegetative activity. The rise in temperature might inhibit growth, but not significantly. Some studies have indicated that moderate warming could enhance the production capacity of plants (Wu et al. 2011, Xu et al. 2013), but warming might also suppress the total production of certain herbaceous plants (Hoeppner & Dukes 2012, Lv et al. 2016). Li & Yang (2014) also suggested that year-round warming exacerbates water deficits in the spring and early summer, thereby damaging vegetation. Further research is necessary to confirm this finding.

3. Varying responses of different vegetation types to climate change

Vegetation phenology is the timing of seasonal events that are considered the result of adaptive responses to environmental conditions. Many researchers have revealed that NDVI changes and phenology showed great variations among different vegetation types (Chuai et al. 2013, Fan et al. 2016, Luo et al. 2009).

Figures 3, 4, and 5 show the variability in phenological shifts (SOS, EOS, and LOS) of the different vegetation types (forest, meadow steppe, typical steppe, and desert steppe), respectively.

The SOS in the forest, meadow, and typical steppe areas with higher biomass exhibited similar trends. According to the meteorological data from every station, increased precipitation promoted the advance of the growing season. However, the temperature effects were not as significant as the precipitation effects. For the EOS, the temperature had a greater influence in the regions with rich biomass (forest and meadow steppe) than did precipitation. The precipitation primarily affected the end of vegetative growth in the arid and semi-arid areas (desert steppe). Generally, depending on the phenological shift (SOS, EOS or LOS), precipitation had a more significant promotional effect on the vegetation growth in most areas, especially in the regions with lower vegetation coverage (typical and desert steppes). However, the differential responses of the vegetation types to meteorology are still not perfectly understood on the Inner Mongolian Plateau (Cui et al.

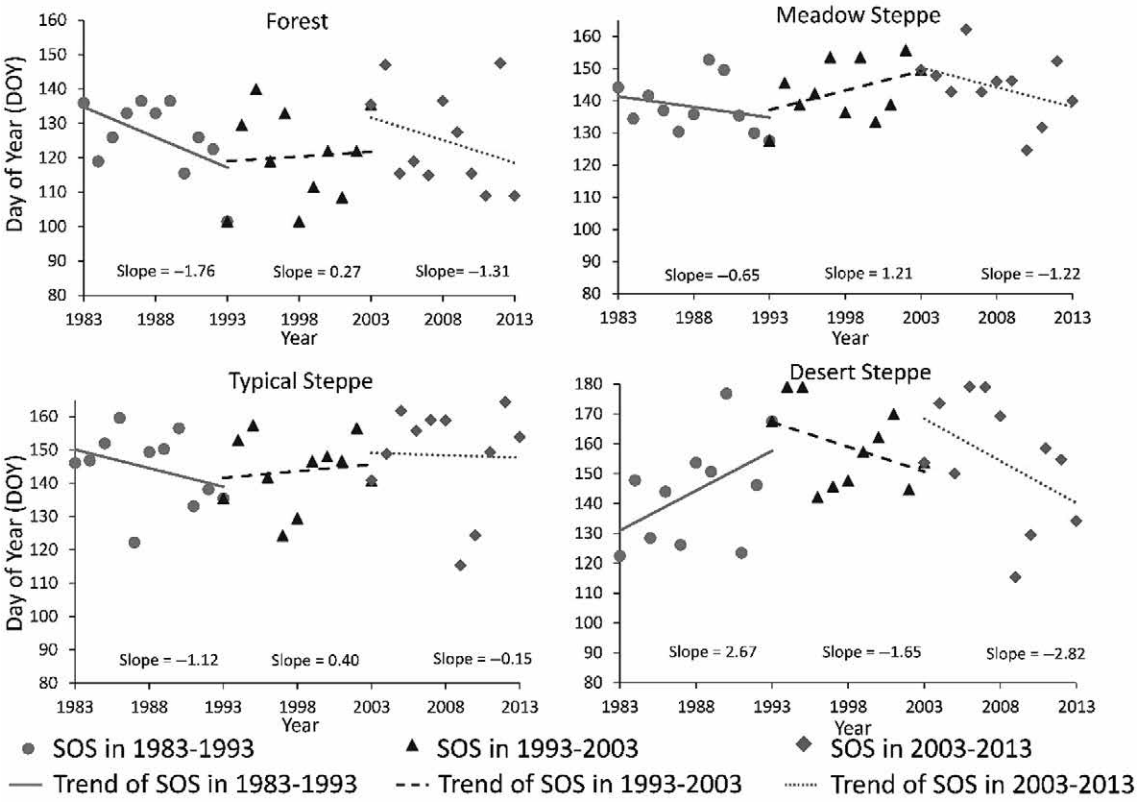

Fig. 3. Start of growing season (SOS) for different vegetation types during 1983-1993 (●), 1993-2003 (▲), and 2003-2013 (♦)

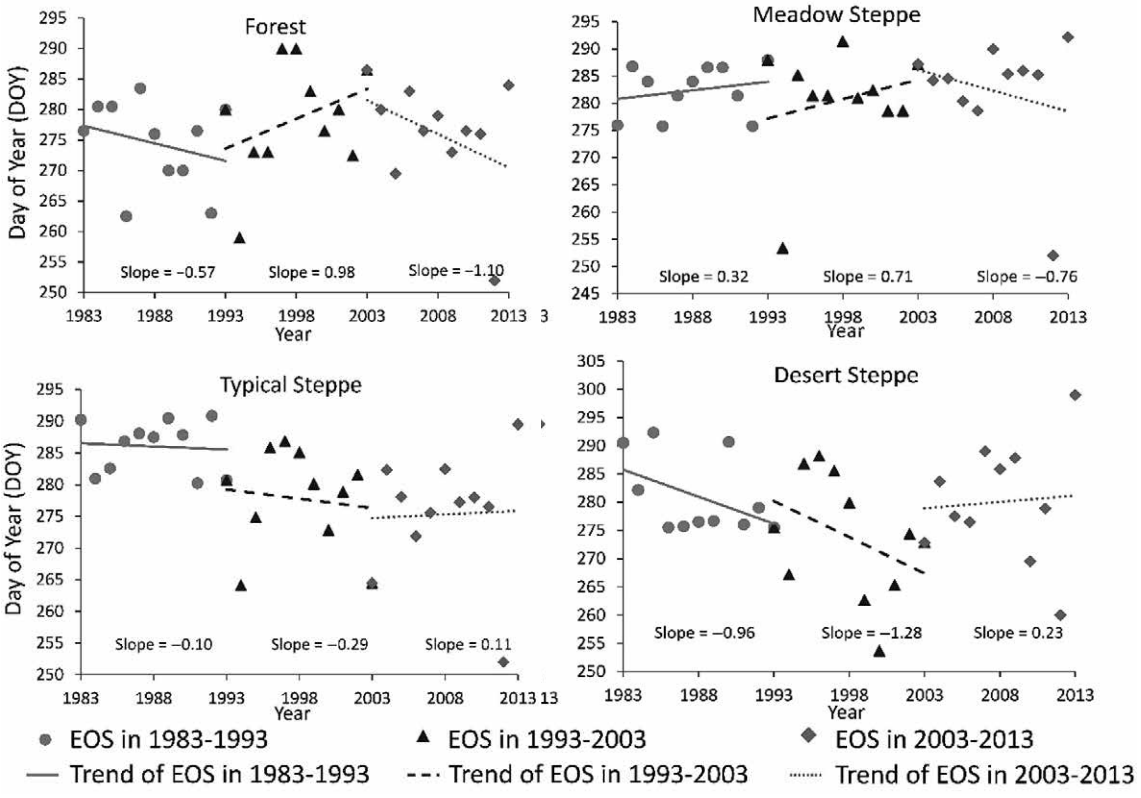

Fig. 4. End of growing season (EOS) for different vegetation types during 1983-1993 (●), 1993-2003 (▲), and 2003-2013 (♦)

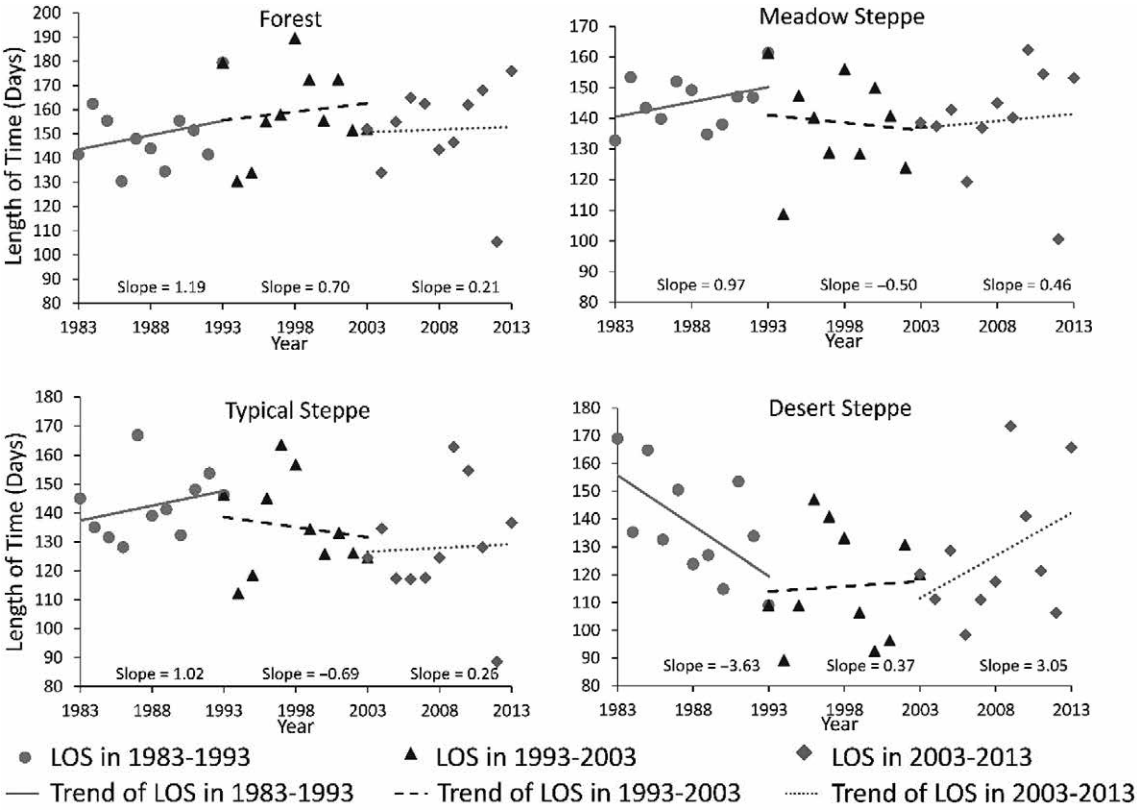

Fig. 5. Length of growing season (LOS) for different vegetation types during 1983-1993 (●), 1993-2003 (▲), and 2003-2013 (♦)

2012, Fan et al. 2016).

The present study has some limitations. Land use and land cover changes have important effects on the grassland ecosystems and policy at regional and global scales (Hu & Nacun 2018). Both are closely related to human activities. In this study, we assessed different land cover types (forest, meadow steppe, typical steppe, desert steppe) in the same manner, but excessive logging and grazing pressure should be different. Thus, more details about land cover change and grassland degradation must be extracted in future studies to achieve sustainable development in Inner Mongolia. From a technical point of view, the method of determining phenology worked well in areas with high vegetation coverage, but was problematic in the desert steppe. Thus, a more suitable method of detecting the phenology should be developed for areas with little vegetation. For the detection of more detailed climate changes in the IMAR, it is necessary to include more meteorological stations in future research. And in future studies, the responses of various vegetation types to climate change should also be analyzed using more *in situ* data.

Conclusions

Based on our results using the longest available NDVI time series, we evaluated the vegetative activity dynamics and phenological shifts in the IMAR. The correlations between the phenological changes (SOS, POS, EOS, and LOS) and meteorology (precipitation and temperature) were also studied. The primary findings can be summarized as follows:

1. The largest degraded area with a decreasing cumulative annual NDVI trend was detected during 1993-2003. A reversal occurred during 2003-2013, when 18.28% of the total vegetation covered area had a significantly increasing trend.
2. Generally, the POS and EOS advanced during the study period in the IMAR. The LOS expanded in the more recent decade.
3. The phenology was closely related with climate changes, especially precipitation in the spring.
4. Increased temperature may inhibit the growth of vegetation.

Overall, our study indicated that vegetative activity was promoted in the most recent decade in the IMAR, and that there was a significant correlation with the climate data. However, our study did not consider land cover and human activities that affect vegetation

productivity and spatial variation. Thus, future studies of the variability in responses of different vegetation types to climate change and human activities will be undertaken.

Acknowledgments

We are grateful to Ms. Yae Kimura and Ms. Wakana Kyuno of the University of Tsukuba, Japan, and to all staff members of the Rangeland Survey and Design Institute of Inner Mongolia, China, for their assistance with the field experiments. This work was supported by the Japan Society for the Promotion of Science (JSPS) Grants-in-Aid for Scientific Research (B) (No. 21405033).

References

Chen, J. et al. (2004) A simple method for reconstructing a high-quality NDVI time-series data set based on the Savitzky-Golay filter. *Remote Sens. Environ*., **91**, 332-344.

Chuai, X. W. et al. (2013) NDVI, temperature and precipitation changes and their relationships with different vegetation types during 1998-2007 in Inner Mongolia, China. *Int. J. Climatol*., **33**, 1696-1706.

Cong, N. et al. (2013) Changes in satellite-derived spring vegetation green-up date and its linkage to climate in China from 1982 to 2010: a multimethod analysis. *Glob. Change. Biol*., **19**, 881-891.

Crosby, D. S. et al. (1996) Inter-satellite calibration using empirical distribution functions. *In* 8th Conference on Satellite Meteorology and Ocean. ed. Meteorological Society, Atlanta, GA, American Meteorological Society, Boston, USA, 188-190.

Cui, L. and Shi, J. (2010) Temporal and spatial response of vegetation NDVI to temperature and precipitation in eastern China. *J. Geogr. Sci*., **20**, 163-176.

Cui, Y. P. et al. (2012) An analysis of temporal evolution of NDVI in various vegetation-climate regions in Inner Mongolia, China. *Procedia Environ. Sci*., **13**, 1989-1996.

Ding, X. H. & Chen, Y. T. (2008) The characteristics of precipitation and temperature in Inner Mongolia for the last 50 years. *Meteorol. J. Inner Mongolia*, **2**, 17-19 [In Chinese].

Editorial Board of Vegetation Map of China, Chinese Academy of Sciences (2007) *Vegetation Map of the People's Republic of China (1:1,000,000).* Geological Press, Beijing, China.

Ellis, J. (1992) The grazing lands of northern China: ecology, society and land use. *In* Grasslands and Grassland Sciences in Northern China: A Report of the Committee on Scholarly Communication with the People's Republic of China Office of International Affairs, ed. The National Research Council. National Academy Press, Washington DC, USA, 9-36.

Fan, Y. et al. (2016) Divergent responses of vegetation aboveground net primary productivity to rainfall pulses in the Inner Mongolian Plateau, China. *J. Arid Environ*., **129**, 1-8.

Gamon, J. A. et al. (2013) Spatial and temporal variation in primary productivity (NDVI) of coastal Alaskan tundra: decreased vegetation growth following earlier snowmelt. *Remote Sens. Environ*., **129**, 144-153.

Gisladottir, G. & Stocking, M. (2005) Land degradation control and its global environmental benefits. *Land Degrad. Dev*., **16**, 99-112.

Glenn, E. P. et al. (2008) Relationship between remotely-sensed vegetation indices, canopy attributes and plant physiological processes: what vegetation indices can and cannot tell us about the landscape. *Sensors*, **8**, 2136-2160.

Gong, Z. et al. (2015) MODIS normalized difference vegetation index (NDVI) and vegetation phenology dynamics in the Inner Mongolia Grassland. *Solid Earth*, **6**, 1185-1194.

Hmimina, G. et al. (2013) Evaluation of the potential of MODIS satellite data to predict vegetation phenology in different biomes: An investigation using ground-based NDVI measurements. *Remote Sens. Environ*., **132**, 145-158.

Hoeppner, S. S. & Dukes, J. S. (2012) Interactive responses of old-field plant growth and composition to warming and precipitation. *Glob. Change Biol*., **18**, 1754-1768.

Hu, J. et al. (2010) Longer growing seasons lead to less carbon sequestration by a subalpine forest. *Glob. Change Biol*., **16**, 771-783.

Hu, Y. & Nacun, B. (2018) An analysis of land-use change and grassland degradation from a policy perspective in Inner Mongolia, China, 1990-2015. *Sustainability*, **10**, 4048.

Jeong, S. et al. (2011) Phenology shifts at start vs. end of growing season in temperate vegetation over the Northern Hemisphere for the period 1982-2008. *Glob. Change Biol*., **17**, 2385-2399.

Jiang, G. et al. (2006) Restoration and management of the Inner Mongolia Grassland require a sustainable strategy. *Ambio*., **35**, 269-270.

John, R. et al. (2008) Predicting plant diversity based on remote sensing products in the semi-arid region of Inner Mongolia. *Remote Sens. Environ*., **112**, 2018-2032.

Kang, L. et al. (2007) Grassland ecosystems in China: review of current knowledge and research advancement. *Philos. Trans. R. Soc. Lond. B. Biol. Sci*., **362**, 997-1008.

Karlsen, S. R. et al. (2008) MODIS-NDVI-based mapping of the length of the growing season in northern Fennoscandia. *Int. J. Appl. Earth Obs. Geoinf*., **10**, 253-266.

Kawamura, K. et al. (2005) Comparing MODIS vegetation indices with AVHRR NDVI for monitoring the forage quantity and quality in Inner Mongolia grassland, China. *Grassl. Sci*., **51**, 33-40.

Kimball, J. S. et al. (2004) Satellite radar remote sensing of seasonal growing seasons for boreal and subalpine evergreen forests. *Remote Sens. Environ*., **90**, 243-258.

Kröpfl, A. I. et al. (2013) Degradation and recovery processes in semi-arid patchy rangelands of northern Patagonia, Argentina. *Land Degrad. Develop*., **24**, 393-399.

Lee, R. et al. (2002) Evaluating vegetation phenological patterns in Inner Mongolia using NDVI time-series analysis. *Int. J. Remote Sens*., **23**, 2505-2512.

Li, A. et al. (2012) Distinguishing between human-induced and climate-driven vegetation changes: a critical application of RESTREND in Inner Mongolia. *Landscape Ecol*., **27**, 969-982.

Li, F. et al. (2013) The response of aboveground net primary productivity of desert vegetation to rainfall pulse in the

temperate desert region of northwest China. *PLOS ONE*, **8**, e73003.

Li, H. & Yang, X. (2014) Temperate dryland vegetation changes under a warming climate and strong human intervention-with a particular reference to the district Xilin Gol, Inner Mongolia, China. *Catena*, **119**, 9-20.

Li, W. et al. (2007) Property rights and grassland degradation: A study of the Xilingol pasture, Inner Mongolia, China. *J. Environ. Manage.*, **85**, 461-470.

Ludwig, J. A. et al. (2000) Monitoring Australian rangeland sites using landscape function indicators and ground and remote-based techniques. *Environ. Monit. Assess.*, **64**, 167-178.

Luo, L. et al. (2009) Research on the correlation between NDVI and climatic factors of different vegetations in the northeast China. *Acta Bot, Boreali-Occident Sin.*, **29**, 800-808.

Lv, X. et al. (2016) Sensitive indicators of zonal Stipa species to changing temperature and precipitation in Inner Mongolia grassland, China. *Front. Plant Sci.*, **7**, 73.

Miao, L. et al. (2015) Vegetation dynamics and factor analysis in arid and semi-arid Inner Mongolia. *Environ. Earth Sci.*, **73**, 2343-2352.

Piao, S. et al. (2006) Variations in satellite-derived phenology in China's temperate vegetation. *Glob. Change Biol.*, **12**, 672-685.

Ravi, S. et al. (2010) Land degradation in drylands: interactions among hydrologic-aeolian erosion and vegetation dynamics. *Geomorphology*, **116**, 236-245.

Rey, A. et al. (2011) Impact of land degradation on soil respiration in a steppe (*Stipa tenacissima* L.) semi-arid ecosystem in the SE of Spain. *Soil Biol. Biochem.*, **43**, 393-403.

Savitzky, A. & Golay, M. J. E. (1964) Smoothing and differentiation of data by simplified least squares procedures. *Anal. Chem.*, **36**, 1627-1639.

Sop, T. K. & Oldeland, J. (2013) Local perceptions of woody vegetation dynamics in the context of a "greening Sahel": a case study from Burkina Faso. *Land Degrad. Develop.*, **24**, 511-527.

Tian, H. et al. (2015) Response of vegetation activity dynamic to climatic change and ecological restoration programs in Inner Mongolia from 2000 to 2012. *Ecol. Eng.*, **82**, 276-289.

Vrieling, A. et al. (2011) Viability of African farming systems from phenological analysis of NDVI time series. *Clim. Chang.*, **109**, 455-477.

Wu, X. & Liu, H. (2013) Consistent shifts in spring vegetation green-up date across temperate biomes in China, 1982-2006. *Glob. Change Biol.*, **19**, 870-880.

Wu, Z. et al. (2011) Responses of terrestrial ecosystems to temperature and precipitation change: a meta-analysis of experimental manipulation. *Glob. Change Biol.*, **17**, 927-942.

Xu, X. et al. (2010) Change in vegetation coverage and its relationships with climatic factors in temperate steppe, Inner Mongolia. *Acta Ecol. Sin.*, **30**, 3733-3743.

Xu, Z. et al. (2013) Interactive effects of elevated CO_2, drought and warming on plants. *J. Plant Growth Regul.*, **32**, 692-707.

Yong-Zhong, S. et al. (2005) Influences of continuous grazing and livestock exclusion on soil properties in a degraded sandy grassland, Inner Mongolia, northern China. *Catena*, **59**, 267-278.

Yu, F. et al. (2003) Response of seasonal vegetation development to climatic variations in eastern central Asia. *Remote Sens. Environ.*, **87**, 42-54.

Zhan, X. et al. (2007) Restoration of *Stipa krylovii* steppes in Inner Mongolia of China: assessment of seed banks and vegetation composition. *J. Arid Environ.*, **68**, 298-307.

Zhang, X. (2007) *Vegetation Map of People's Republic of China*. Geological Publishing House, Beijing, China.

Zhao, H. et al. (2006) Effects of desertification on soil and crop growth properties in Horqin sandy cropland of Inner Mongolia, north China. *Soil Tillage Res.*, **87**, 175-185.

Zhou, H. et al. (2009) Detecting the impact of the "Grain for Green" program on the mean annual vegetation cover in Shaanxi province, China using SPOT-VGT NDVI data. *Land Use Policy*, **26**, 954-960.